Published in final edited form as:
IEEE ASME Trans Mechatron. 2013 January 3; 18(4): 1413–1418. doi:10.1109/TMECH.2012.2235077.

Magnetically Actuated Soft Capsule With the Multimodal Drug Release Function

Sehyuk Yim, **Kartik Goyal**, and **Metin Sitti**
Department of Mechanical Engineering, Carnegie Mellon University, Pittsburgh, PA 15213 USA

Sehyuk Yim: samy@cmu.edu; Kartik Goyal: kartik.goyal11@gmail.com; Metin Sitti: sitti@cmu.edu

Abstract

In this paper, we present a magnetically actuated multimodal drug release mechanism using a tetherless soft capsule endoscope for the treatment of gastric disease. Because the designed capsule has a drug chamber between both magnetic heads, if it is compressed by the external magnetic field, the capsule could release a drug in a specific position locally. The capsule is designed to release a drug in two modes according to the situation. In the first mode, a small amount of drug is continuously released by a series of pulse type magnetic field (0.01–0.03 T). The experimental results show that the drug release can be controlled by the frequency of the external magnetic pulse. In the second mode, about 800 mm^3 of drug is released by the external magnetic field of 0.07 T, which induces a stronger magnetic attraction than the critical force for capsule's collapsing. As a result, a polymeric coating is formed around the capsule. The coated area is dependent on the drug viscosity. This paper presents simulations and various experiments to evaluate the magnetically actuated multimodal drug release capability. The proposed soft capsules could be used as minimally invasive tetherless medical devices with therapeutic capability for the next generation capsule endoscopy.

Index Terms

Capsule endoscope; drug delivery; magnetic micro-robot; medical robotics

I. Introduction

Current medical technologies are developing toward minimally invasive diagnosis and therapy. Magnetic capsule endoscopy is one of the state-of-the-art medical technologies to represent this trend. Many research groups have demonstrated the magnetic maneuvering of an endoscopic capsule inside a human body or a swine's gastrointestinal (GI) tract [1]–[4]. Although their performance should be improved for application in clinics, recent advances in magnetic manipulation would allow a stable 3-D motion control of the magnetic capsule endoscopes in the near future [4], [5].

Color versions of one or more of the figures in this paper are available online at http://ieeexplore.ieee.org.

The next challenge of active capsule endoscopy is to integrate therapeutic capabilities. Various drug-releasing capsules have been developed. Richert *et al.* proposed a magnetic capsule, which is disassembled by an external magnetic field [6]. Xitian *et al.* proposed a remote controlled capsule activated by magnetic repulsive force, frequency signal, and thermal expansion [7], [8]. These drug-releasing capsules showed feasibility in the experiments. Currently, some capsules are being used for the research on the drug-absorption rate of each organ. The intelSite capsule (Innovative Devices, Raleigh, NC) uses on-board shape memory alloys to open the drug-releasing holes [9], [10]. The Enterion capsule (Phaeton research, Nottingham, U.K.) employs a spring–piston mechanism actuated by a highly efficient radio-frequency signal [11]. However, considering that the mechanical configuration of these drug-releasing capsules is complicated and they require too much space, the aforementioned mechanisms are not ideal for magnetic capsule endoscopes.

In the previous research, we proposed a magnetically actuated soft capsule endoscope (MASCE) platform with potential capabilities for drug releasing, biopsy, and palpation [12]–[14]. As a follow-up study, this paper presents its advanced design to perform multimodal drug release. As the outline of this paper, Section II introduces the working principle of the localized drug-release mechanism and simulations. In Section III, the targeting performance of the proposed drug-releasing mechanism is evaluated. In Section IV, limitations of the proposed mechanism are discussed.

II. Drug Release Mechanism

A. Design and Characterization

Fig. 1 shows the application scenario of the drug-releasing magnetic capsule. After the capsule is magnetically guided to a desired position, it is compressed by the enhanced external magnetic field. The drug-containing chamber is situated between two heads with internal magnets. The drug inside the chamber is released through four slits at the corners by the preloading force of the upper head during compression. Fig. 2(a) shows a CAD model of the designed prototype (see Table I for the specifications of the prototype). The detailed configuration of MASCE was introduced in [12]. Because the chamber is made of a soft elastomer, the slits are opened only under the external load. The drug is injected through a small hole in the ceiling of the chamber. The drug chamber is clamped under the upper head and sealed once integrated into the MASCE. Fig. 2(b) shows the characterized shape deformation curve (the length change of the capsule versus the external magnetic attraction), which is divided into three sections. The first section is between the point O and the point A. In this region, the chamber is compressed as the applied force increases. If the external permanent magnet repeats the linear reciprocal motion, due to a series of pulse-type external magnetic field, the capsule releases the drug slowly and continuously. The second section is from the point A to the point B. A large volume of the drug is released and the area around the target is coated by the released drug. The last section is from the point B to the point C. In this region, a little drug is released while the chamber skin is pressed.

According to the capsule design, the distance between the chamber and the head at the other side is about 2–3 mm. If the capsule is erected, the upper head contacts the drug chamber due to its weight. The results of indentation tests [see the blue X marks in Fig. 2(b)] were

obtained by the capsule in the air. If the chamber is filled with a viscous drug and the capsule is indented in the water, the chamber's stiffness becomes higher because the drug chamber becomes a damper and the internal pressure of the drug chamber should be higher than the ambient water pressure. In this case, the gradient of the plot between the point O and the point A [see Fig. 2(b)] becomes smaller. This initial stiffness prevents the undesired drug release during capsule's locomotion.

The proposed chamber design has two improvements as compared with [12]. First, the drug is released via four slits at the corners of the chamber, which allows a natural inflow of the ambient fluid to the chamber after the drug release. Because the chamber's shape is recovered by the inflow, the drug release can be repeated multiple times. Next, the chamber has four slits at its corners, which are toward the space between side linkages. As a result, the waste of the drug in the polymeric coating mode can be minimized.

B. Analysis

Fig. 3(a) shows the drug release mechanism using simplified diagrams. The chamber's collapsing is accelerated as it is compressed because the upper internal magnet is attracted to the lower one at a short distance. This critical condition can be used to implement the drug release in two different modes. In this section, the multimodal drug release is simulated in detail. The simulations of multimodal drug release have two assumptions; drug chamber volume as a function of the external magnetic attraction and the applied magnetic force as a function of time. Fig. 3(b) shows the drug chamber volume as a function of the external magnetic attraction, which is assumed considering the shape deformation curve and recovery curve [see Fig. 2(b)] and the specification (see Table I). The drug chamber has a critical force F_{cr} before being fully collapsed. For example, if the applied preload force is 1.35 N, the chamber volume reduces from 800 to 120 mm^3.

The profile of the applied magnetic force is set as in Fig. 4(a). A series of weak stimulation in the regions A and B are for small and continuous drug release. Their maximum force (0.5 N) is weaker than the critical force F_{cr} of Fig. 3(b). In the region B, the frequency becomes doubled, but the magnetic attraction is same as in the region A. The stimulation in the region C is for imparting a local drug coating. The maximum force (1.4 N) is stronger than the critical force.

If the applied magnetic force at each time [see Fig. 4(a)] is plugged into the shape deformation and recovery curve [see Fig. 3(b)], the chamber volume at each time is interpolated as in Fig. 4(b). In the part A and B, the drug release is almost continuous. If the frequency of the external magnetic field becomes higher, the chamber volume plot becomes more fluctuated. In the part C, the stimulation induces the full compression of the chamber. At the moment, the drug release speed becomes extremely high. Using such high fluidic force, the drug coating is formed around the target. As the drug release is repeated, the concentration of the released drug becomes lower because of the inflow of the ambient fluid [see Fig. 4(c)]. Considering the lowering of the concentration, the actual quantity of the released drug per time in A and B are 195 and 265 mm^3/s, respectively.

III. Experiments

A. Multiple Drug Release

The performance of the multimodal drug release was evaluated in experiments. A mixture of water and Methylene blue was injected into the drug chamber of the capsule, which was then placed in a container filled with water. The images of the drug-releasing capsule were taken by a camera above the water container [see Fig. 5(a)]. The magnetic capsule was stimulated by the external magnetic field. The field magnitude (0.01 T < B_{max} < 0.07 T) and the frequency (0.1 Hz < f < 2 Hz) were differently set. The external permanent magnet (cylindrical, diameter 50 mm × length 80 mm, the maximum remanence $B_{r,\ max}$ = 1.4 T) was moved manually toward the magnetic capsule until the mechanical limit is reached. The distance (h) between the external magnet and the capsule was measured. The magnetic field was interpolated based on the magnetic field versus distance curve, which was measured by a magnetometer (model 410, Lake Shore, Westerville, OH). The average frequency was calculated by taken images.

Fig. 6(a)–(c) shows some snapshots of the magnetic capsule in the multiple drug release. Key observations are as follows.

1. *Maximum magnetic field:* As simulated in Fig. 4, the compression of the chamber is controlled by only the maximum magnetic field. The magnetic capsule promptly reacts to the change in the external magnetic field. During both the compression and the relaxation process, delayed response due to the mass inertia of the upper head is not observed. One important point is that the compressed chamber does not necessarily result in a drug release if the viscosity of the injected drug is high. The viscous drug is not diffused after being released and then, if the chamber is relaxed, the released drug flows back into the chamber.
2. *Frequency:* Even though the magnetic field governs the compression of the chamber, adjusting the frequency of the external magnetic field is useful to control the drug release rate. It is extremely difficult to prove this relation directly using experiments because measuring the volume of the released drug in 3-D is not possible. Therefore, the performance of the multiple drug release experiment is evaluated by 2-D image analysis indirectly even though it is affected by the diffusion of the releasing drug. Fig. 6(d) shows the area coated by the diffusing drug as a function of the time. B_{max} was maintained at 0.03 T and the frequency was differently set (1.2 Hz < f < 2.0 Hz). The plots show the external magnetic field of high frequency induces a fast diffusion of the released drug.

B. Polymeric Drug Coating

Differing from the first mode, in the polymeric drug-coating mode, even a highly viscous drug can be released because the abrupt compression of the drug chamber gives a strong fluidic force to the squeezed drug. Considering that most drugs for mucus layer protection would be highly viscous, such performance would be useful for the stomach ulcer treatment. However, the physical features of the polymeric coating (e.g., coating area, pattern, and distance) are also important because the polymeric film should be a protection layer.

Therefore, in the next experiments, we investigated the effect of the drug viscosity on the polymeric coating. A mucoadhesive material was used to change the viscosity (see Table II for detailed information of the drug). A total of four hydro-gel samples (M_1–M_4) with different viscosities were prepared (see Table III for detailed information of the hydro-gel samples). The pattern and the area of the released drug at the final state are important points. Using the taken images and imaging processing, they were calculated. Table IV shows the coated area of the released drug and the average distance from the center of the capsule to the coating area. For example, in the case of the M_4, about 317 mm^2 is coated by the polymeric drug, and the average distance is about 8 mm.

The objective of local polymeric coating is to separate a gastric ulcer from an invasive gastric acid and, finally, to guide the tissue's self-healing. Therefore, the biological response of a cell in the proposed clinical scenario needs to be investigated. An epidermal tissue was picked from a human mouth and dyed with an eosin. The dyed cell was placed on a slide-glass surrounded by a polydimethyl siloxane (PDMS) wall. After dyeing, the cell was exposed to HCl. The behavior of the cell was monitored by an inverted optical microscope. Fig. 8(a) shows the response of the cell without a polymeric coating. The cytoplasm of the cell swells as soon as exposed to HCl because the cytoplasm which had been dried on the glass substrate, absorbs the water of HCl solution. Next, if the cell is coated by a hydro-gel, the cytoplasm of the cell shrinks as soon as exposed to HCl [see Fig. 8(b)]. This is because the osmotic pressure makes the water in the cytoplasm move to the HCl solution. Finally, if the cell-coating material is a nonhydro material like silicone-oil, there is no interaction between the cytoplasm and the HCl solution [see Fig. 8(c)]. This means that the cell is completely separated from the external HCl solution. The aforementioned results show that the drug for the protection of the tissue should be a nonhydro gel.

IV. Discussion

Multimodal drug release was demonstrated in the experiments, but the designed magnetic capsule also has two potential issues in future clinical applications. First, if the proposed mechanism is implemented in a swallowable capsule (diameter: 10 mm; length: 30 mm, volume: 2300 mm^3), the drug chamber occupies about 30% of the total capsule volume; according to the experiments, the drug chamber volume should be at least 800 mm^3 to cover the targeted tissue. Considering that the next generation capsule endoscopes should be equipped with other functional modules such as biopsy and biosensors as well, such space assignment might not be practical. As the second issue, in the local polymeric coating mode, the coating drug is formed around the target, not at the target. For example, Fig. 7 shows that four areas are separately formed. These issues remain to be solved in future work. One possible solution for the first issue is to assemble the drug chamber with the main capsule in the stomach after inserting separately.

V. Conclusion

In this paper, a MASCE with a multimodal drug release function is proposed. In the first mode, a small amount of drug is continuously released by a series of pulse type magnetic field (0.01–0.03 T and 1.2–2 Hz). The diffusion of the released drug in 2-D images was

analyzed and the results show that the drug release rate can be modulated by the frequency of the external magnetic pulse. In future clinical applications, this mode would be useful when multiple diseased tissues are observed at different positions during endoscopy. In the second mode, 800 mm^3 of drug is released by the external magnetic field of 0.07 T, which induces a stronger magnetic attraction than the capsule's critical force. As a result, a viscous polymeric coating is formed around the target. The coated area is dependent on the drug viscosity. In the case of viscous drug (viscosity: 0.2 Pa·s), the coated area is about 317 mm^2. Such soft capsules with localized drug release function would be used to treat gastric ulcer in a minimally invasive manner in the future.

Acknowledgments

This work was supported in part by the National Institutes of Health under Grant R01-NR014083.

The authors would like to thank H. Chung and N. R. Wash-burn for synthesizing the mucoadhesive polymers and the members of the NanoRobotics Laboratory for their continuous feedback and suggestions.

References

1. Swain P, Toor A, Vodke F, Keller J, Gerber J, Rabinovitz E, Rothstein RI. Remote magnetic manipulation of a wireless capsule endoscope in the esophagus and stomach of humans. Gastrointest Endos. Jun; 2010 71(7):1290–1293.
2. Rey JF, Ogata H, Hosoe N, Ohtsuka K, Ogata N, Ikeda K, Aihara H, Pangtay I, Hibi T, Kudo S, Tajiri H. Feasibility of stomach exploration with a guided capsule endoscope. Endos. 2010; 42(7): 541–545.
3. Volke F, Keller J, Schneider A, Gerber J, Reimann-Zawadzki M, Rabinovitz E, Mousse CA, Swain P. *In vivo* remote manipulation of modified capsule endoscopes using an external magnetic field. Gastrointest Endos. 2008; 67:AB121–AB122.
4. Carpi F, Kastelein N, Talcott M, Pappone C. Magnetically controllable gastrointestinal steering of video capsules. IEEE Trans Biomed Eng. Feb; 2011 58(2):231–234. [PubMed: 20952324]
5. Mathieu J, Beaudoin G, Martel S. Method of propulsion of a ferromagnetic core in the cardiovascular system through magnetic gradients generated by an MRI system. IEEE Trans Biomed Eng. Feb; 2006 53(2):292–299. [PubMed: 16485758]
6. Richert H, Surzhenko O, Wangemann S, Heinrich J, Gornet P. Development of a magnetic capsule as a drug release system for future applications in the human GI tract. J Magn Magn Mater. May; 2005 293(1):497–500.
7. Xitian P, Xialin Z, Chenglin P, Wenchen H, Hongying L. A novel remote controlled capsule for human drug absorption studies. Proc 27th Annu Int Conf Eng Med Biol Soc. 2005:5066–5068.
8. Xitian P, Hongying L, Kang W, Yulin L, Xiaolin Z, Zhiyu W. A novel remote controlled capsule for site-specific drug delivery in human GI tract. Int J Pharmaceutics. 2009; 382(1):160–164.
9. Mummaneni V, Doll W, Sandefer E, Page R, Ryo U, Digenis G, Kaul S. Gamma scintigraphic evaluation of the intestinal absorption of stavudine in healthy male volunteers using InteliSite® capsule. Pharm Sci. 1999; 9(1):608–611.
10. Mcgirr ME, Mcallister SM, Peter EE, Vickers AW, Parr AF, Basit AW. The use of the intelSite companion device to deliver mucoadhesive polymer to the dog colon. Eur J Pharm Sci. 2009; 36(4):386–391. [PubMed: 19063965]
11. Fuhr U, Staib AH, Harder S, Becker K, Liermann D, Schöllnhammer G, Roed IS. Absorption of ipsapirone along the human gastrointestinal tract. Br J Clin Pharmacol. 1994; 38:83–86. [PubMed: 7946942]
12. Yim S, Sitti M. Design and rolling locomotion of a magnetically actuated soft capsule endoscope. IEEE Trans Robot. Feb; 2012 28(1):183–194.

13. Yim S, Sitti M. Shape-programmable soft capsule robots for semi-implantable drug delivery. IEEE Trans Robot. 2012; 28(5):1198–1202.

14. Yim, S.; Sitti, M. 3-D localization method for a magnetically actuated soft capsule endoscope and its applications. under review

15. [Online]. Available: http://web2.airmail.net/uthman/specimens/index.html

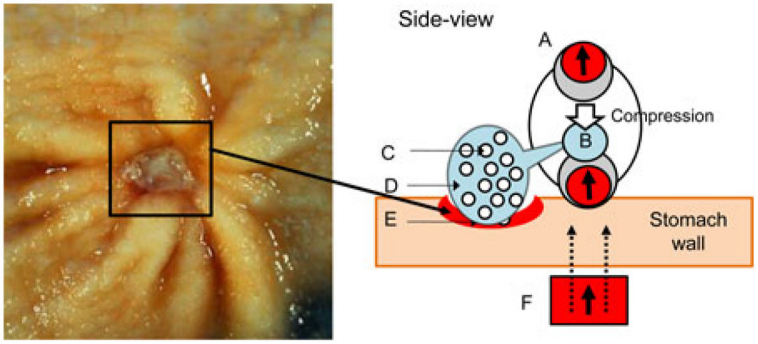

Fig. 1.

Application scenario of MASCE for localized drug release. MASCE is axially contracted by the external magnetic field next to the ulcer. The drug chamber is compressed by the upper head (see the white arrow). A: MASCE with two internal magnets. B: Drug chamber. C: Cytoprotective agent. D: Polymer. E: Diseased tissue (e.g., gastric ulcer and image source from [15]). F: External Permanent Magnet (EPM). The black arrows mean the magnetization direction of the magnets. The dotted black lines represent the external magnetic field.

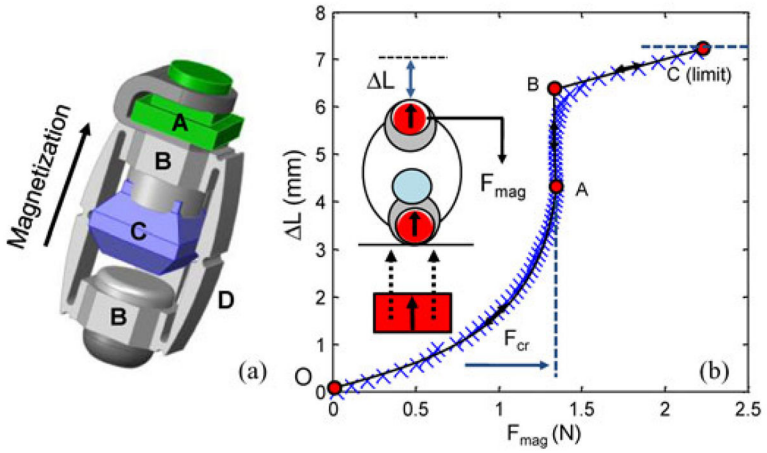

Fig. 2.

(a) CAD model of the soft capsule for multimodal drug release. A: camera module. B: heads with internal magnets. C: drug chamber. D: side-linkages. (b) Shape deformation and recovery curve of the prototype. The blue X-marks mean the results of indentation tests. The capsule is compressed by the external magnetic attraction following the route (O–A–B–C) during the full compression. At A, the chamber is abruptly collapsed by the external force, which is the critical force (F_{cr}: 1.34 N). The actual drug release is completed at the point B.

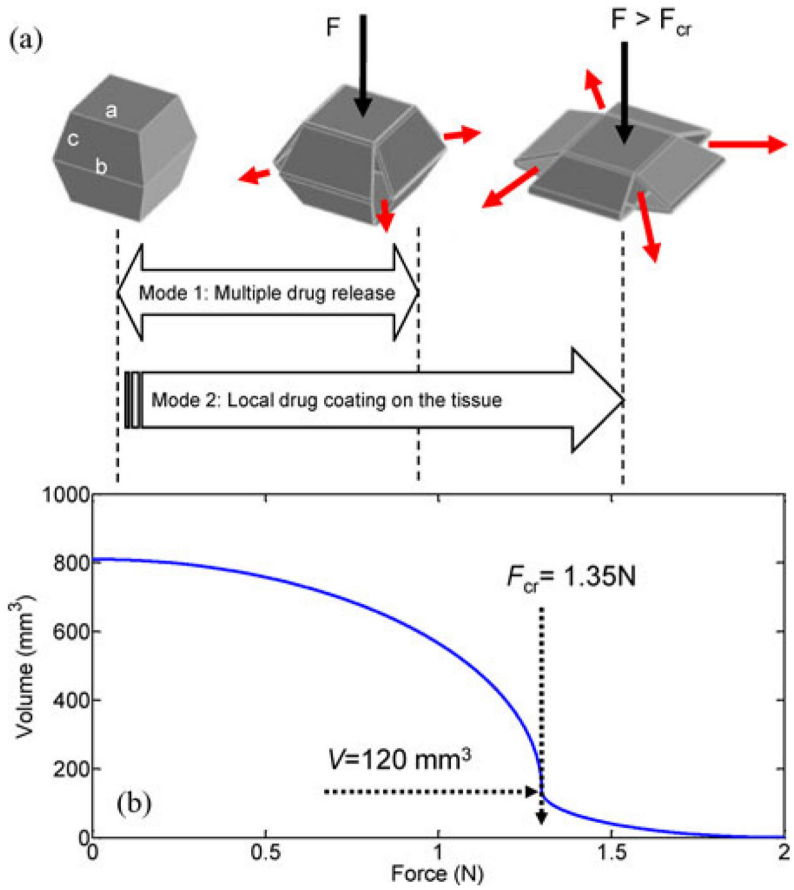

Fig. 3.

(a) Multimodal drug release mechanism. *Mode1*: the chamber can maintain its shape under the preloading force weaker than F_{cr}. In this range, a small amount of the drug can be pumped out of the chamber, repeatedly. *Mode 2*: Due to the internal magnetic attraction, the chamber is collapsed by the external magnetic attraction over the critical force. This abrupt collapsing causes a large volume of drug to be released. (b) Simulation assumptions (see the blue solid line): the volume of the chamber as a function of stimulation (force).

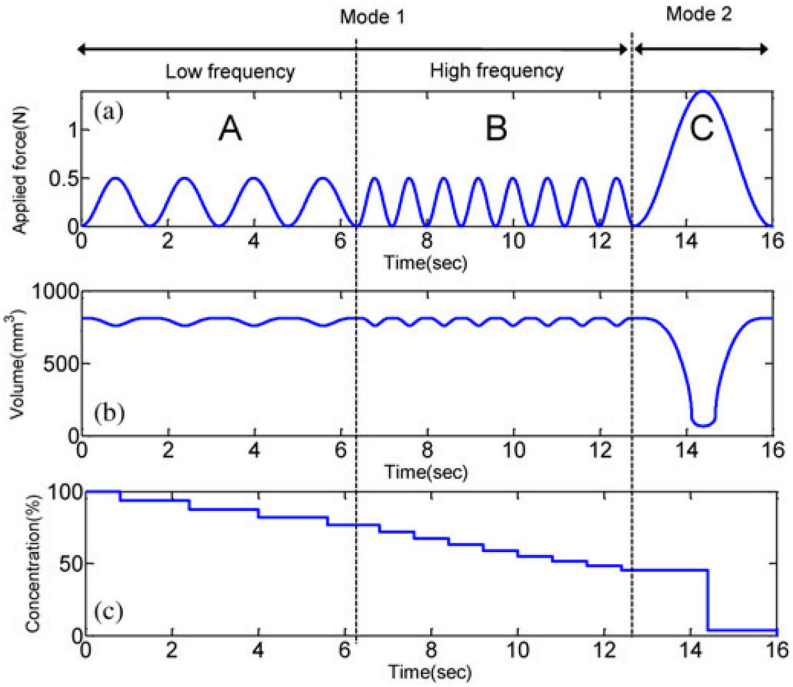

Fig. 4.

Simulated multimodal drug release by different external magnetic field. (a) *Assumption*: Applied force stimulations on the chamber. A: $f = 0.62$ Hz and $f = 1.25$ Hz. (b) *Result*: Volume change as a function of time due to the applied force. (c) Concentration of the drug in the chamber.

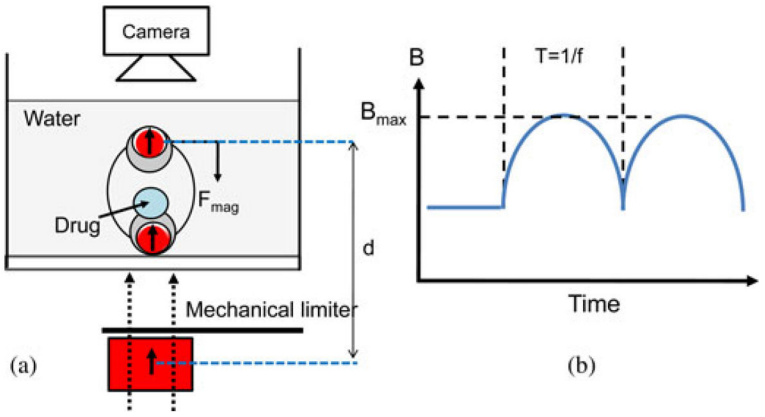

Fig. 5.

(a) Schematic of the experimental setup to evaluate drug release pattern. (b) Variables of the stimulation. B_{max}: The maximum magnetic field and f: the frequency.

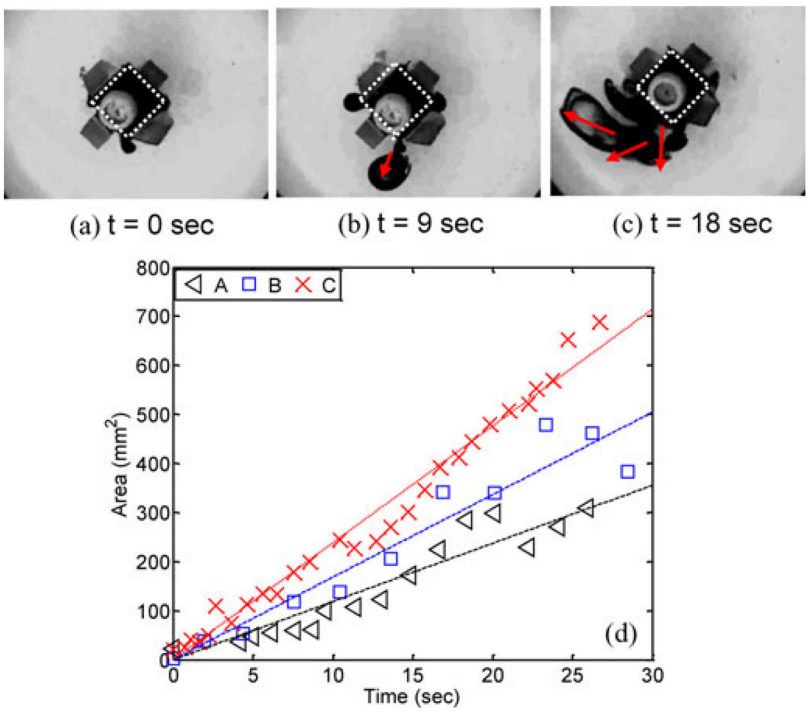

Fig. 6.

(a)–(c) Snapshots of the released drug. The white dotted line means the area of the drug chamber. The red arrow means the diffusion direction of the released drug; f = 1.6 Hz; B_{max} = 0.03 T. (d) Drug-coated area versus time; the frequency of the external magnetic field: A: 1.2 Hz; B: 1.6 Hz; C: 2.0 Hz. B_{max} = 0.03 T.

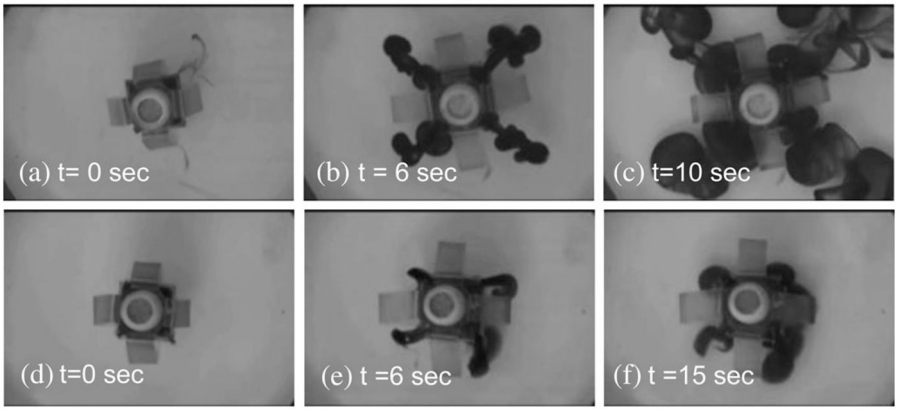

Fig. 7.

Top-view snapshots of the local polymeric coating demonstration (B_{max} = 0.07 T). (a)–(c) Low viscosity sample (M_1). (d)–(f) High viscosity sample (M_4).

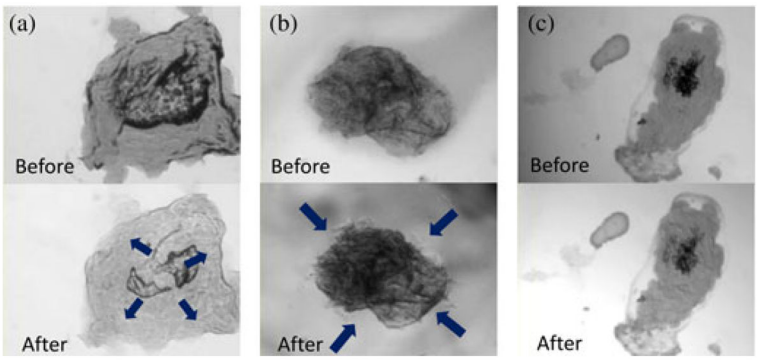

Fig. 8.

Optical microscopic images of the HCl exposure experiments. (a) Direct exposure to HCl. (b) Indirect exposure to HCl after coated by hydro-gel polymer. (c) Indirect exposure to HCl after coated by a silicone-oil. The attached multimedia file shows the response of the cells more clearly.

TABLE I

Specifications of the Prototype

Diameter of capsule head (initial/compressed)	15 mm/20 mm
Length (initial/compressed)	40 mm/30 mm
Mass	6.0 g
Internal Magnets:	
Size (cylindrical)	Diameter: 8 mm; Length: 8 mm
Material	NdFeB
Drug chamber	
Height	8.2 mm
Length* (side surface)	*a*: 7.6 mm; *b*: 12 mm, *c*: 4.1 mm
Volume	800 mm^3

*See Fig. 3(a) for the design variables of the side surface.

TABLE II

Material Property of the Sample Drugs

Formula	$C_3H_4O_2$
Ratio	Carbopol: 0.3%
	Poly-vinyl-pyrrolidone (PVP): 10%
	Glycol solution: 0.6%
pH	7.1
Viscosity (Pa·s)	2.0 at the shear rate of 1 sec^{-1}
	0.1 at the shear rate of 10 sec^{-1}

TABLE III

Specifications of the Hydro-Gel Samples

Material	Mixing ratio (= water:drug)	* Viscosity (Pa s)
M_1	2:3	0.1 – 0.01
M_2	1:2	0.1 – 0.02
M_3	1:4	0.1 – 0.05
M_4	1:6	0.2 – 0.10

* Shear rate dependent: viscosity at 1.0 sec^{-1} and 10.0 sec^{-1} Viscosity measured by Bohlin meter.

TABLE IV

Experimental Results: Drug-Coated Area and Average Distance

Material	Viscosity (Pa s)	* Area (mm^2)	* Distance (mm)
M_1	0.1 – 0.01	4050 (±1391)	33.0 (±14.0)
M_2	0.1 – 0.02	2710 (±1023)	21.3 (±12.8)
M_3	0.1 – 0.05	1225 (±157)	13.3 (±9.2)
M_4	0.2 – 0.10	317 (±47)	7.9 (±5.0)

* Experiments were conducted three times each.